Journal of Naval Architecture and Marine Engineering
December, 2008
DOI: 10.3329/jname.v5i2.2694 http://www.banglajol.info

THERMAL RADIATION EFFECTS ON MHD FREE CONVECTION FLOW PAST AN IMPULSIVELY STARTED VERTICAL PLATE WITH VARIABLE SURFACE TEMPERATURE AND CONCENTRATION

S. Suneetha[1], N. Bhaskar Reddy[1] and V. Ramachandra Prasad[2]

[1]Department of Mathematics, Sri Venkateswara University, Tirupati - 517502, A. P., INDIA,
Email: suneetha_svu@yahoo.com
[2]Professor of Applied Mathematics, Department of Mathematics, MITS, Madanapalle, A. P, INDIA
Email: rcpmaths@mits.ac.in

Abstract

Thermal radiation effects on hydromagnetic free convection flow past an impulsively started vertical plate with variable surface temperature and concentration is analyzed, by taking into account the heat due to viscous dissipation. The governing boundary layer equations of the flow field are solved by an implicit finite difference method of Crank-Nicholson type. A parametric study is performed to illustrate the influence of radiation parameter, magnetic parameter, Grashof number, Prandtl number, Eckert number on the velocity, temperature and concentration profiles. Also, the local and average skin-friction coefficient, Nusselt number and Sherwood number are presented graphically. The numerical results reveal that an increase in thermal radiation reduces both the velocity and temperature in the boundary layer and a rise in viscous dissipation accelerates the flow.

Key words: Thermal radiation, MHD, viscous dissipation, vertical plate.

NOMENCLATURE

B_0	magnetic induction
cp	specific heat at constant pressure
C'	dimensional species concentration
C	dimensionless species concentration
D	species diffusion coefficient
Ec	Eckert number
g	acceleration due to gravity
Gr	thermal Grashof number
Gm	solutal Grashof number
k	thermal conductivity
k_e	mean absorption coefficient
m	exponent in power law variation of the wall temperature
M	magnetic parameter
n	exponent in power law variation of the concentration
N	radiation parameter
Nu_X	local Nusselt number
$\overline{Nu}$	average Nusselt number
Pr	Prandtl number
q_r	radiation heat flux
Sc	Schmidt number
Sh_X	local Sherwood number
$\overline{Sh}$	average Sherwood number
t'	dimensional time
t	dimensionless time
T'	dimensional temperature
T	dimensionless temperature
u_0	velocity of the plate
u, v	velocity components in x, y directions respectively
U, V	dimensionless velocity components in X, Y directions respectively
x, y	dimensional coordinates along and normal to the plate respectively
X, Y	dimensionless coordinates along and normal to the plate respectively

Greek symbols

α	thermal diffusivity
β	volumetric coefficient of thermal expansion
β^*	volumetric coefficient of expansion with concentration
μ	dynamic viscosity
ν	kinematic viscosity
ρ	density of the fluid
σ	electrical conductivity
σ_s	Stefan-Boltzmann constant
τ'	dimensional local skin-friction coefficient

 Received on: 1 Oct. 2008

τ_X dimensionless local skin- friction coefficient

$\overline{\tau}$ dimensionless average skin-friction coefficient

Subscripts

w conditions on the wall

∞ free stream conditions

1. Introduction

In the processes involving high temperatures, the radiation heat transfer in combination with conduction, convection and also mass transfer plays very important role in the design of pertinent equipments in the areas such as nuclear power plants, gas turbines and the various propulsion devices for air crafts, missiles, satellites and space vehicles. Chamkha et al. (2001) studied the radiation effects on the free convection flow past a semi-infinite vertical plate with mass transfer. Muthucumaraswamy and Senthil Kumar (2004) investigated the heat and mass transfer effects on moving vertical plate in the presence of thermal radiation. Prasad et al. (2007) considered the radiation and mass transfer effects on a two-dimensional flow past an impulsively started isothermal vertical plate. The interaction of radiation with hydromagnetic flow has become industrially more prominent in the processes wherever high temperatures occur. Takhar et al. (1996) analyzed the radiation effects on MHD free convection flow past a semi-infinite vertical plate using Runge-Kutta Merson quadrature**.** Abd-El-Naby et al. (2003) studied the radiation effects on MHD unsteady free-convection flow over a vertical plate with variable surface temperature**.** Chaudhary et al. (2006) studied the radiation effect with simultaneous thermal and mass diffusion in MHD mixed convection flow from a vertical surface. Ramachandra Prasad et al. (2006) studied the transient radiative hydromagnetic free convection flow past an impulsively started vertical plate with uniform heat and mass flux.

Viscous mechanical dissipation effects are very important in geophysical flows and also in certain industrial operations and are usually characterized by the Eckert number. Mahajan and Gebhart (1989) reported the influence of viscous heating dissipation in natural convective flows, showing that the heat transfer rates are reduced by an increase in the dissipation parameter. The influence of viscous dissipation and radiation on an unsteady MHD free-convection flow past an infinite heated vertical plate in a porous medium with time-dependent suction was studied by Israel-Cookey et al. (2003). **R**ecently Zueco (2007) used Network Simulation method [NSM] to study the effects of viscous dissipation and radiation on unsteady MHD free convection flow past a vertical porous plate.
The object of this paper is to analyze the interaction of radiation and mass transfer on the free convection flow of an electrically conducting dissipative fluid past an impulsively started isothermal vertical plate with variable surface temperature and concentration.

2. Mathematical Analysis

An unsteady two-dimensional laminar natural convection flow of a viscous incompressible electrically conducting, radiating and dissipative fluid past an impulsively started semi-infinite vertical plate with variable surface temperature and concentration is considered. The fluid is assumed to be gray, absorbing-emitting but non-scattering. The flow model and physical coordinate system are shown in Fig.1.
The x-axis is taken along the plate in the upward direction and the y-axis is taken normal to it. A uniform magnetic field is applied transversely to the direction of the flow. The fluid is assumed to be slightly conducting and hence the magnetic Reynolds number is much less than unity and the induced magnetic field is negligible in comparison with the transverse applied magnetic field. Initially, it is assumed that the plate and the fluid are at the same temperature T'_∞ and concentration level C'_∞ everywhere in the fluid. At time t'>0, the plate starts moving impulsively in the vertical direction with constant velocity u_0 against the gravitational field. Also, it is assumed that at t'>0, the plate temperature and concentration near the plate are raised to $T' = T'_\infty + \left(T'_w - T'_\infty\right) x^m$, $C' = C'_\infty + \left(C'_w - C'_\infty\right) x^n$ respectively and are maintained constantly thereafter. It is assumed that the concentration C' of the diffusing species in the binary mixture is very less in comparison to the other chemical species which are present and hence the Soret and Dufour effects are negligible. It is also assumed that there is no chemical reaction between the diffusing species and the fluid. Then, under the usual Boussinesq's approximation, in the absence of an input electric field, the governing boundary layer equations are

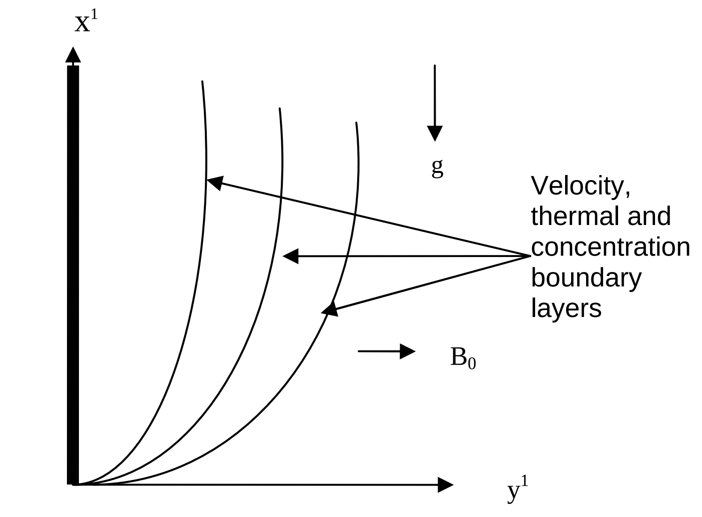

Fig.1. Physical model and coordinate system.

Continuity equation

$$\frac{\partial u}{\partial x}+\frac{\partial v}{\partial y}=0 \tag{1}$$

Momentum equation

$$\frac{\partial u}{\partial t'}+u\frac{\partial u}{\partial x}+v\frac{\partial u}{\partial y}=g\,\beta\,(T'-T'_\infty)+g\,\beta^*\,(C'-C'_\infty)+\nu\,\frac{\partial^2 u}{\partial y^2}-\frac{\sigma\,B_0^2}{\rho}u \tag{2}$$

Energy equation

$$\frac{\partial T'}{\partial t'}+u\frac{\partial T'}{\partial x}+v\frac{\partial T'}{\partial y}=\alpha\,\frac{\partial^2 T'}{\partial y^2}-\frac{1}{\rho\,c_p}\frac{\partial q_r}{\partial y}+\frac{\nu}{c_p}\left(\frac{\partial u}{\partial y}\right)^2 \tag{3}$$

Species equation

$$\frac{\partial C'}{\partial t'}+u\frac{\partial C'}{\partial x}+v\frac{\partial C'}{\partial y}=D\frac{\partial^2 C'}{\partial y^2} \tag{4}$$

The initial and boundary conditions are

$$\begin{aligned}
&t'\le 0: u=0,\;\; v=0,\;\; T'=T'_\infty,\;\; C'=C'_\infty\\
&t'>0: u=u_0,\;\; v=0,\;\; T'=T'_\infty+\left(T'_w-T'_\infty\right)x^m,\;\; C'=C'_\infty+\left(C'_w-C'_\infty\right)x^n \quad at \quad y=0\\
&\qquad u=0,\; v=0,\; T'=T'_\infty,\; C'=C'_\infty \qquad at \quad x=0\\
&\qquad u\to 0, T'\to T'_\infty,\;\; C'\to C'_\infty \qquad as \quad y\to\infty
\end{aligned} \tag{5}$$

By using the Rosseland approximation (Brewster [1992]), the radiative heat flux q_r is given by

$$q_r=-\frac{4\sigma_s}{3k_e}\frac{\partial T'^4}{\partial y} \tag{6}$$

It should be noted that by using the Rosseland approximation, the present analysis is limited to optically thick fluids. If temperature differences within the flow are sufficiently small, then Equation (6) can be linearized by expanding T'^4 into the Taylor series about T'_∞, which after neglecting higher order terms takes the form

$$T'^4\cong 4T'^3_\infty\,T'-3T'^4_\infty \tag{7}$$

In view of Equations (6) and (7), Equation (3) reduces to

$$\frac{\partial T'}{\partial t'}+u\frac{\partial T'}{\partial x}+v\frac{\partial T'}{\partial y}=\alpha\,\frac{\partial^2 T'}{\partial y^2}+\frac{16\sigma_s T'^3_\infty}{3k_e\rho\,c_p}\frac{\partial^2 T'}{\partial y^2}+\frac{\nu}{c_p}\left(\frac{\partial u}{\partial y}\right)^2 \tag{8}$$

In order to write the governing equations and the boundary conditions in dimensionless form, the following non-dimensional quantities are introduced.

$$X = \frac{x u_0}{\nu}, \quad Y = \frac{y u_0}{\nu}, \quad t = \frac{t' u_0^2}{\nu}, \quad U = \frac{u}{u_0}, \quad V = \frac{v}{u_0}$$

$$Gr = \frac{\nu g \beta (T'_w - T'_\infty)}{u_0^3}, \quad Gm = \frac{\nu g \beta^* (C'_w - C'_\infty)}{u_0^3}, \quad N = \frac{k_e k}{4\sigma_s T'^3_\infty}, M = \frac{\sigma B_0^2 \nu}{u_0^2} \tag{9}$$

$$T = \frac{T' - T'_\infty}{T'_w - T'_\infty} \quad C = \frac{C' - C'_\infty}{C'_w - C'_\infty}, \quad \Pr = \frac{\nu}{\alpha}, \quad Sc = \frac{\nu}{D}, \quad Ec = \frac{u_o^2}{c_p (T'_w - T'_\infty)}$$

Now Equations (1), (2), (8) and (4) are reduced to the following non-dimensional form

$$\frac{\partial U}{\partial X} + \frac{\partial V}{\partial Y} = 0 \tag{10}$$

$$\frac{\partial U}{\partial t} + U \frac{\partial U}{\partial X} + V \frac{\partial U}{\partial Y} = Gr\, T + Gm\, C + \frac{\partial^2 U}{\partial Y^2} - MU \tag{11}$$

$$\frac{\partial T}{\partial t} + U \frac{\partial T}{\partial X} + V \frac{\partial T}{\partial Y} = \frac{1}{\Pr}\left(1 + \frac{4}{3N}\right)\frac{\partial^2 T}{\partial Y^2} + Ec\left(\frac{\partial u}{\partial y}\right)^2 \tag{12}$$

$$\frac{\partial C}{\partial t} + U \frac{\partial C}{\partial X} + V \frac{\partial C}{\partial Y} = \frac{1}{Sc}\frac{\partial^2 C}{\partial Y^2} \tag{13}$$

The corresponding initial and boundary conditions are

$$\begin{aligned} & t \le 0 : U = 0, \; V = 0, \; T = 0, \; C = 0 \\ & t > 0 : U = 1, \; V = 0, \; T = X^m, C = X^n \quad at \quad Y = 0 \\ & \qquad U = 0, \; T = 0, \; C = 0 \quad at \quad X = 0 \\ & \qquad U \to 0, T \to 0, \; C \to 0 \quad as \quad Y \to \infty \end{aligned} \tag{14}$$

For the type of flow under consideration , the local as well as average values of skin-friction coefficient, Nusselt number and Sherwood number are important, which in non-dimensional form are given by

$$\tau_X = \frac{\tau'}{\rho u_0^2} = -\left(\frac{\partial U}{\partial Y}\right)_{Y=0}, \qquad \bar{\tau} = -\int_0^1 \left(\frac{\partial U}{\partial Y}\right)_{Y=0} dX \tag{15}$$

$$Nu_X = -X\left[\left(\frac{\partial T}{\partial Y}\right)_{Y=0} \Big/ T_{Y=0}\right], \qquad \overline{Nu} = -\int_0^1 \left[\left(\frac{\partial T}{\partial Y}\right)_{Y=0} \Big/ T_{Y=0}\right] dX \tag{16}$$

$$Sh_X = -X\left[\left(\frac{\partial C}{\partial Y}\right)_{Y=0} \Big/ C_{Y=0}\right], \qquad \overline{Sh} = -\int_0^1 \left[\left(\frac{\partial C}{\partial Y}\right)_{Y=0} \Big/ C_{Y=0}\right] dX \tag{17}$$

3. Numerical Technique

In order to solve the unsteady, non-linear, coupled Equations (10) - (13) under the conditions (14), an implicit finite difference scheme of Crank-Nicholson type has been employed. The finite difference equations corresponding to Equations (10) - (13) are as follows:

$$\frac{\left[U_{i,j}^{n+1} - U_{i-1,j}^{n+1} + U_{i,j}^{n} - U_{i-1,j}^{n} + U_{i,j-1}^{n+1} - U_{i-1,j-1}^{n+1} + U_{i,j-1}^{n} - U_{i-1,j-1}^{n}\right]}{4\Delta X} + \frac{\left[V_{i,j}^{n+1} - V_{i,j-1}^{n+1} + V_{i,j}^{n} - V_{i,j-1}^{n}\right]}{2\Delta Y} = 0 \tag{18}$$

$$\frac{\left[U_{i,j}^{n+1} - U_{i,j}^{n}\right]}{\Delta t} + U_{i,j}^{n} \frac{\left[U_{i,j}^{n+1} - U_{i-1,j}^{n+1} + U_{i,j}^{n} - U_{i-1,j}^{n}\right]}{2\Delta X} + V_{i,j}^{n} \frac{\left[U_{i,j+1}^{n+1} - U_{i,j-1}^{n+1} + U_{i,j+1}^{n} - U_{i,j-1}^{n}\right]}{4\Delta Y} =$$

$$Gr\, \frac{\left[T_{i,j}^{n+1} + T_{i,j}^{n}\right]}{2} + Gm\, \frac{\left[C_{i,j}^{n+1} + C_{i,j}^{n}\right]}{2} + \frac{\left[U_{i,j-1}^{n+1} - 2U_{i,j}^{n+1} + U_{i,j+1}^{n+1} + U_{i,j+1}^{n+1} - 2U_{i,j}^{n} + U_{i,j+1}^{n}\right]}{2(\Delta Y)^2} \tag{19}$$

$$-M\, \frac{\left[U_{i,j}^{n+1} + U_{i,j}^{n}\right]}{2}$$

$$\frac{[T_{i,j}^{n+1}-T_{i,j}^{n}]}{\Delta t}+U_{i,j}^{n}\frac{\left[T_{i,j}^{n+1}-T_{i-1,j}^{n+1}+T_{i,j}^{n}-T_{i-1,j}^{n}\right]}{2\Delta X}+V_{i,j}^{n}\frac{\left[T_{i,j}-T_{i,j-1}^{n+1}+T_{i,j+1}^{n}-T_{i,j-1}^{n}\right]}{4\Delta Y}=$$

$$\frac{1}{\Pr}\left(1+\frac{4}{3N}\right)\frac{\left[T_{i,j-1}^{n+1}-2T_{i,j}^{n+1}+T_{i,j+1}^{n+1}+T_{i,j-1}^{n}-2T_{i,j}^{n}+T_{i,j+1}^{n}\right]}{2(\Delta Y)^2}+Ec\left[\frac{\left[U_{i,j+1}^{n}-U_{i,j}^{n}\right]}{\Delta Y}\right]^2 \quad (20)$$

$$\frac{[C_{i,j}^{n+1}-C_{i,j}^{n}]}{\Delta t}+U_{i,j}^{n}\frac{\left[C_{i,j}^{n+1}-C_{i-1,j}^{n+1}+C_{i,j}^{n}-C_{i-1,j}^{n}\right]}{2\Delta X}+V_{i,j}^{n}\frac{\left[C_{i,j+1}^{n+1}-C_{i,j-1}^{n+1}+C_{i,j+1}^{n}-C_{i,j-1}^{n}\right]}{4\Delta Y}=$$

$$\frac{1}{Sc}\frac{\left[C_{i,j-1}^{n+1}-2C_{i,j}^{n+1}+C_{i,j+1}^{n+1}+C_{i,j-1}^{n}-2C_{i,j}^{n}+C_{i,j+1}^{n}\right]}{2(\Delta Y)^2} \quad (21)$$

The region of integration is considered as a rectangle with sides $X_{\max}$ (=1) and $Y_{\max}$ (=14), where $Y_{\max}$ corresponds to $Y = \infty$, which lies very well outside the momentum, energy and concentration boundary layers. The maximum of *Y* was chosen as 14 after some preliminary investigations so that the last two of the boundary conditions of Equation (14) are satisfied. Here, the subscript *i*-designates the grid point along the *X*-direction, *j* -along the *Y*-direction and the superscript *n* along the *t*-direction. An appropriate mesh sizes considered for the calculation are ΔX = 0.05, ΔY = 0.25,and the time step is taken as $\Delta t = 0.01$.During any one time step, the coefficients $U_{i.j}^{n}$ and $V_{i.j}^{n}$ appearing in the difference equations are treated as constants. The values of *C*, *T*, *U* and *V* at time level (*n+1*) using the known values at previous time level (*n*) are calculated as follows.

The finite difference Equation (21) at every internal nodal point on a particular *i*-level constitute a tridiagonal system of equations, which is solved by using Thomas algorithm as discussed in Carnahan et al.(1969). Thus, the values of *C* are known at every internal nodal point on a particular *i* at $(n+1)^{th}$ time level . Similarly, the values of *T* are calculated from Equation (20). Using the values of *C* and *T* at $(n+1)^{th}$ time level in Equation (19), the values of *U* at $(n+1)^{th}$ time level are found in similar manner. Then the values of *V* are calculated explicitly using Equation (18) at every nodal point at particular *i*-level at $(n+1)^{th}$ time level. This process is repeated for various *i*-levels. Thus the values of *C, T, U* and *V* are known at all grid points in the rectangular region at $(n+1)^{th}$ time level. Computations are carried out until the steady state is reached. The steady-state solution is assumed to have been reached, when the absolute differences between the values of *U* as well as temperature *T* and concentration *C* at two consecutive time steps are less than 10^{-5} at all grid points.

The derivatives involved in Equations (15) - (17) are evaluated using five-point approximation formula and then the integrals are evaluated using Newton-Cotes closed integration formula.
The truncation error in the finite difference approximation is $O(\Delta t^2+\Delta Y^2+\Delta X)$ and it tends to zero as Δt, ΔY and ΔX tend to zero. Hence the scheme is compatible. The finite difference scheme is unconditionally stable (Ramachandra Prasad et al.(2007)). Stability and compatibility ensure convergence.

4. Results and Discussions

In order to get a physical insight into the problem, extensive computations have been performed for the effects of the controlling thermofluid and hydrodynamic parameters on the dimensionless velocity, temperature and concentration and also on the local and average skin- friction, Nusselt number and Sherwood number. These computational results are shown in Figs. 2-15.

In order to ascertain the accuracy, results from present study are compared with those from previous study. The velocity profiles for *Pr* = 0.71, *Sc* = 0.6, 0.94, *N* = 3.0, *M* = 1.0 are compared with that of Prasad et al. (2007) in Fig.2. It is observed that the present results are in good agreement with that of Prasad et al. (2007).

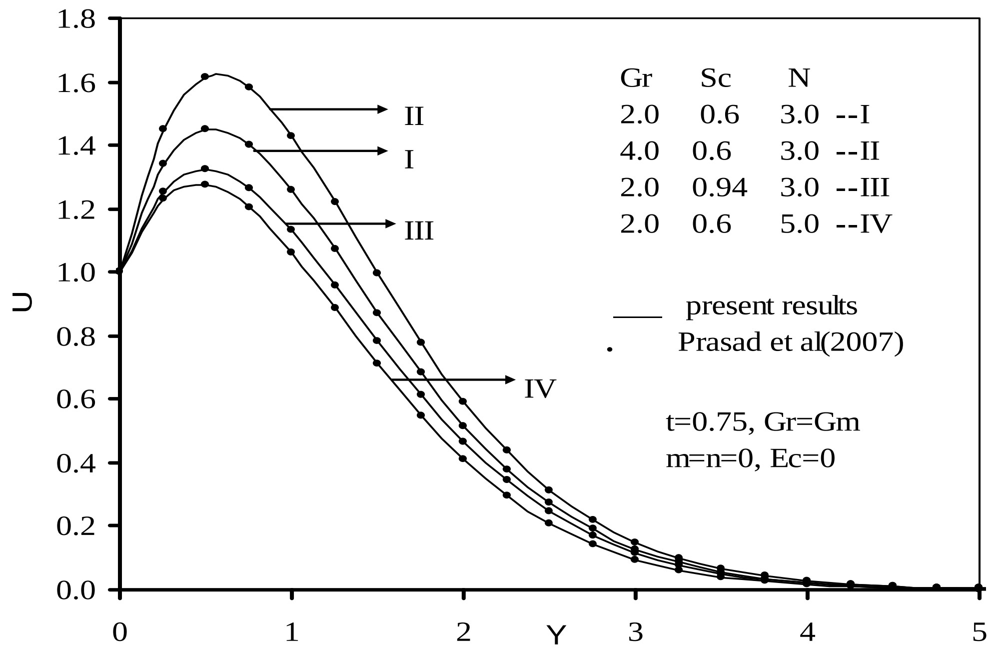

Fig.2: Transient velocity profiles at *X*=1.0 for different *Gr*, *Sc* and *N*

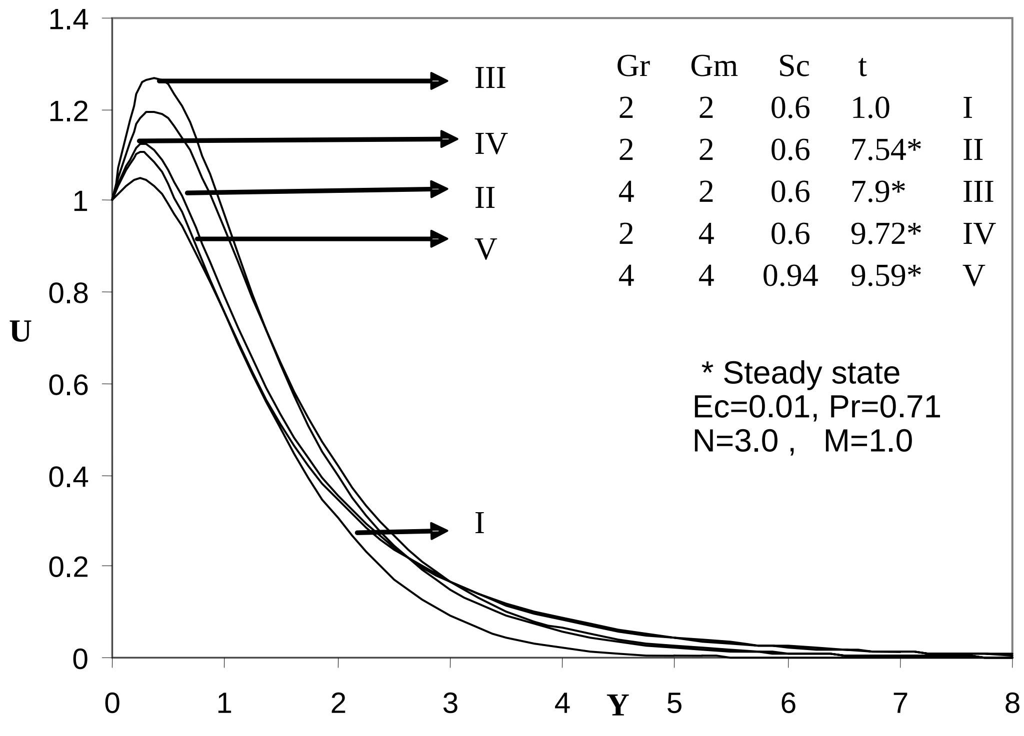

Fig.3: Velocity profiles for different values of *Gr,Gm, and Sc*

Figs. 3 and 6 depict the velocity and temperature profiles for different values of *Gr* and *Gm.* The thermal Grashof number *Gr* signifies the relative effect of the thermal buoyancy (due to density differences) force to the viscous hydrodynamic force in the boundary layer flow. The positive values of *Gr* correspond to cooling of the plate by natural convection. Heat is therefore conducted away from the vertical plate into the fluid which increases temperature and thereby enhances the buoyancy force. It is observed that the transient velocity accelerates due to enhancement in the thermal buoyancy force, i.e., free convection effects. The solutal Grashof number *Gm* defines the ratio of the species buoyancy force to the viscous hydrodynamic force. It is noticed that the transient velocity increases considerably with a rise in the species buoyancy force. In both the cases it is interesting to note that as *Gr* or *Gm* increases, there is a rapid rise in the velocity near the surface of vertical plate and then descends smoothly to the free stream velocity. An increase in *Gr* or *Gm* induces a sizeable decrease in the temperature throughout the boundary layer. The temperature profiles descend smoothly from their maxima of unity at the plate (*Y*=0) to zero at the edge of the boundary layer. The Schmidt number *Sc* embodies the ratio of the momentum diffusivity to the mass (species) diffusivity. It physically relates the relative thickness of the hydrodynamic boundary layer and mass-transfer (concentration) boundary layer. It is observed that as the Schmidt number increases the transient velocity decreases. (Fig. 3).

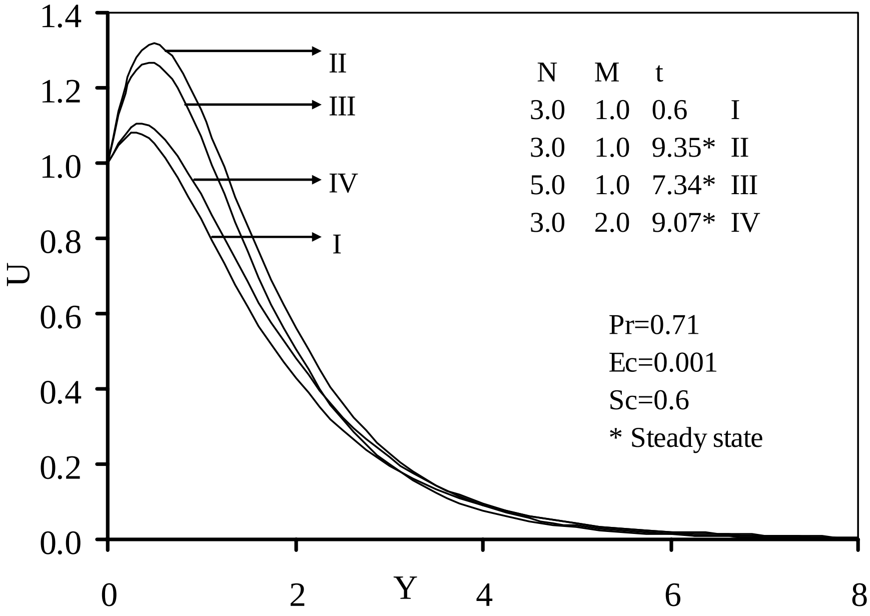

Fig. 4: Velocity profiles for different values of *N* and *M*

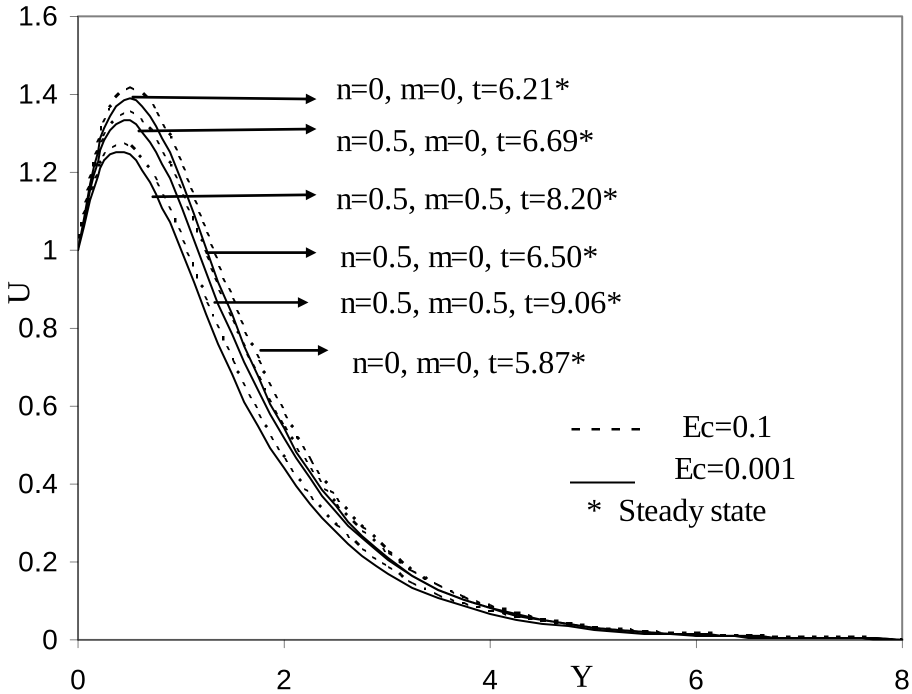

Fig. 5: Steady state velocity profiles for different values of *n* and *m*

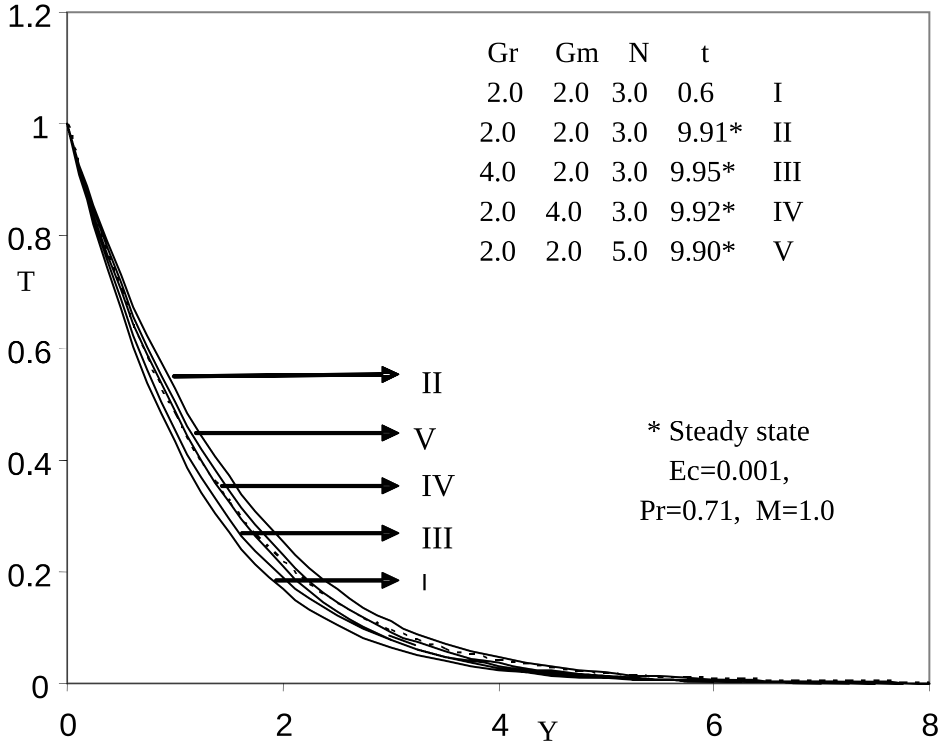

Fig.6: Temperature profiles for different *Gr*, *Gm* and *N*

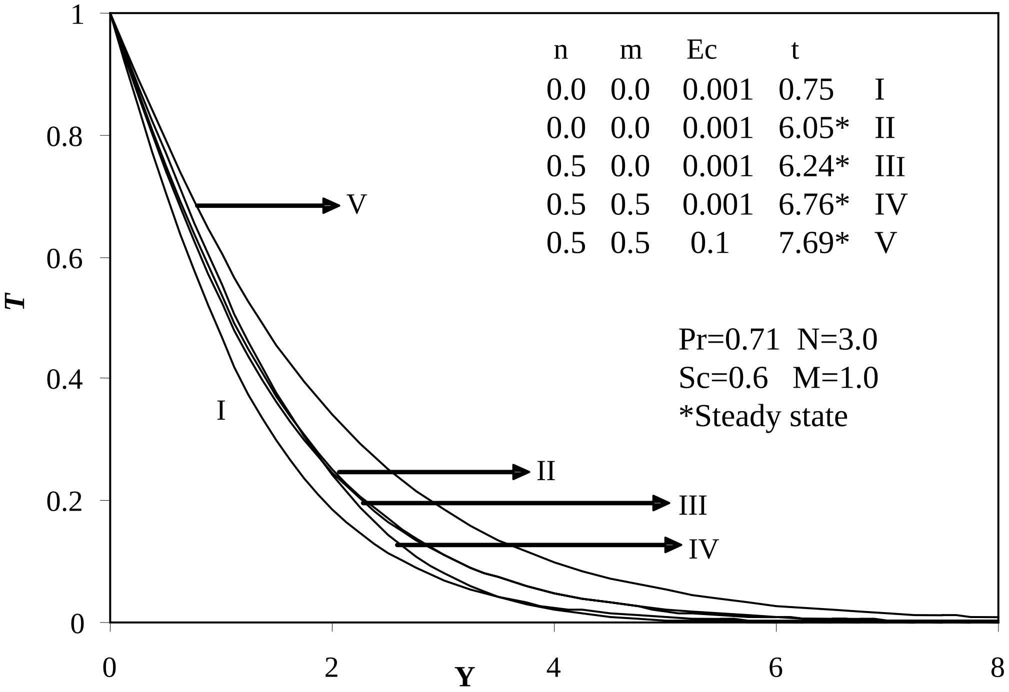

Fig.7: Temperature profiles for different *m*, *n* and *Ec*.

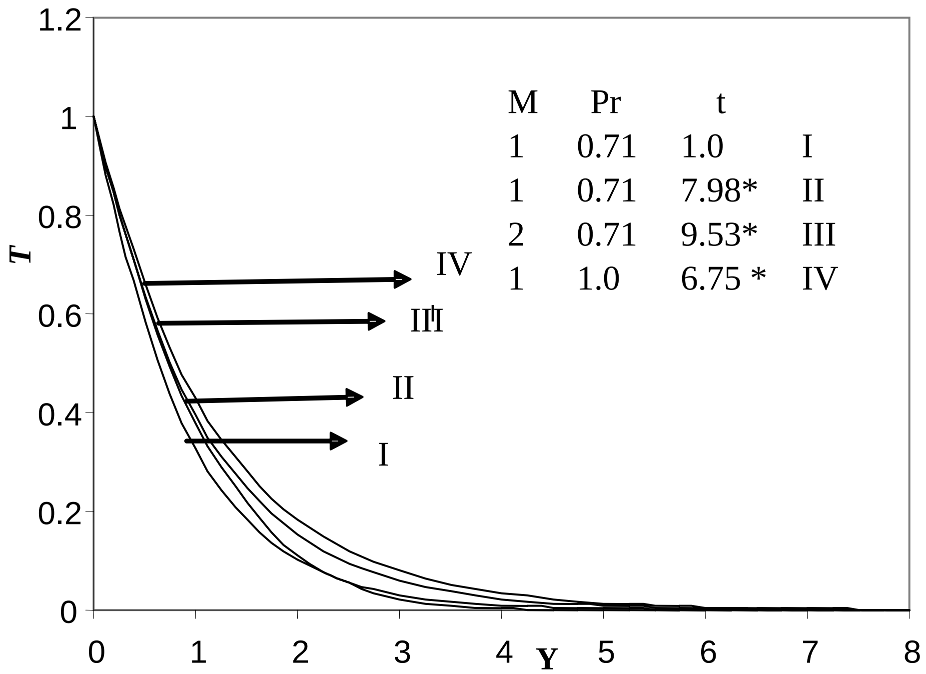

Fig.8. Temperature profiles for different values of *M* and *Pr*

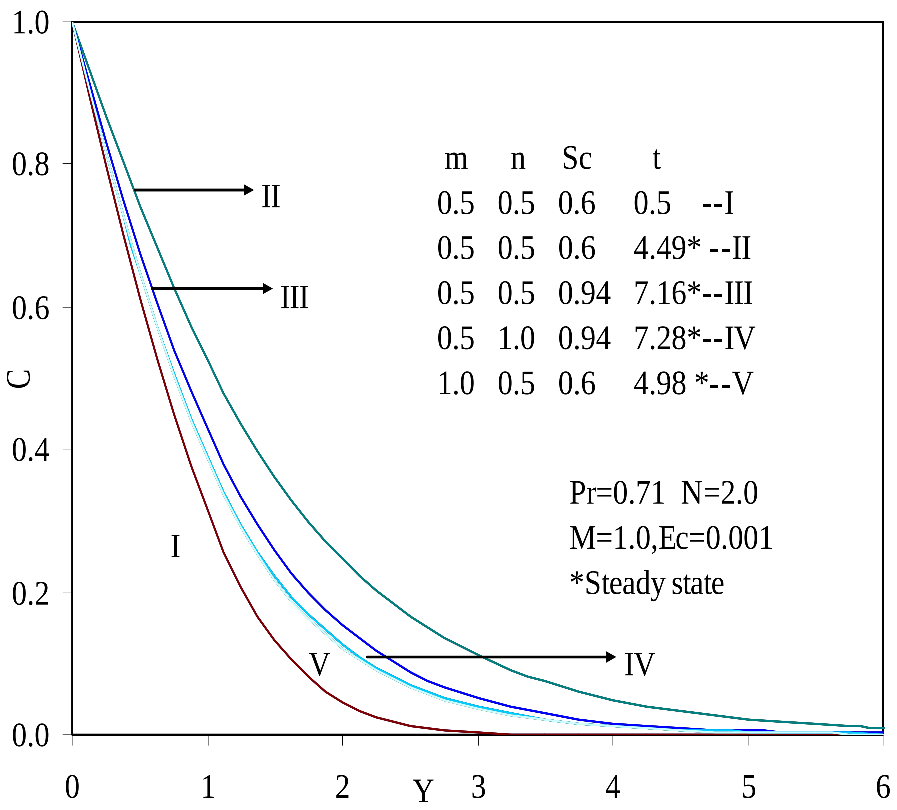

Fig. 9: Transient concentration profiles for different values of *m*, *n* and *Sc*

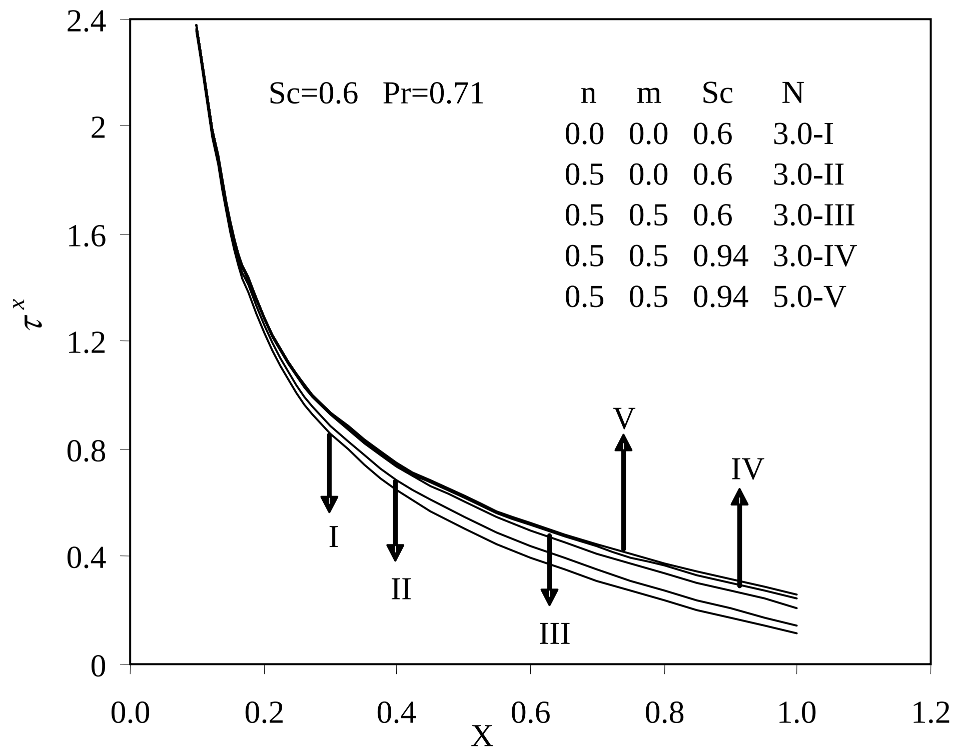

Fig.10 Local skin friction for different values of *n, m, Sc* and *N*

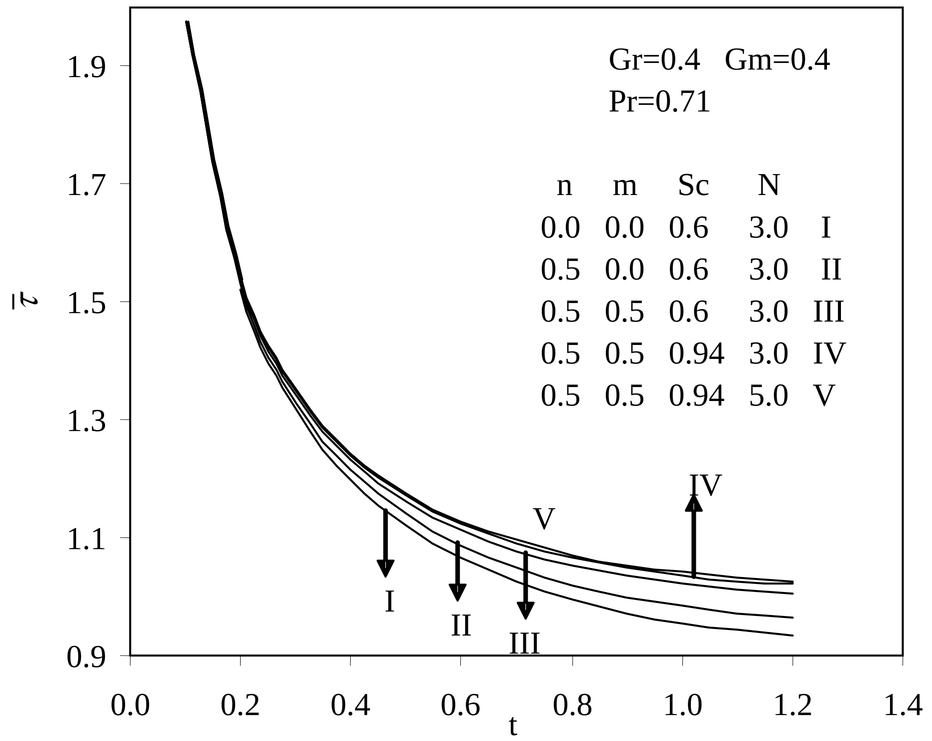

Fig.11. Average skin friction for different *n, m, Sc* and *N*

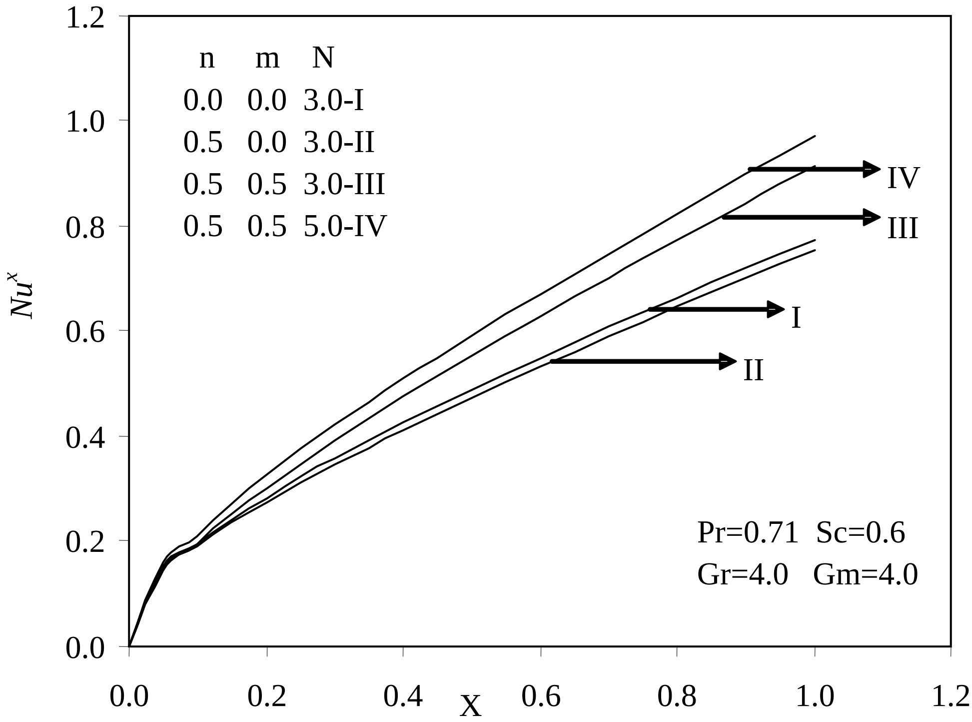

Fig.12: Local Nusselt number for various values of *n, m* and *N*

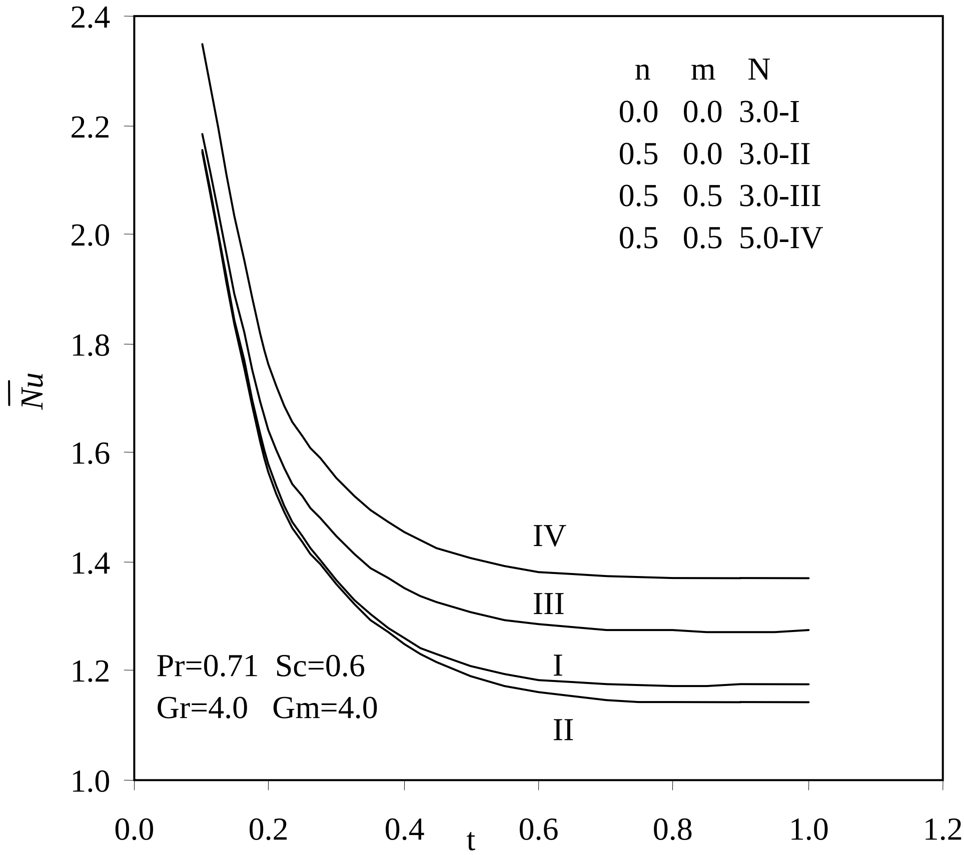

Fig.13 Average Nusselt number for different *n, m* and *N*

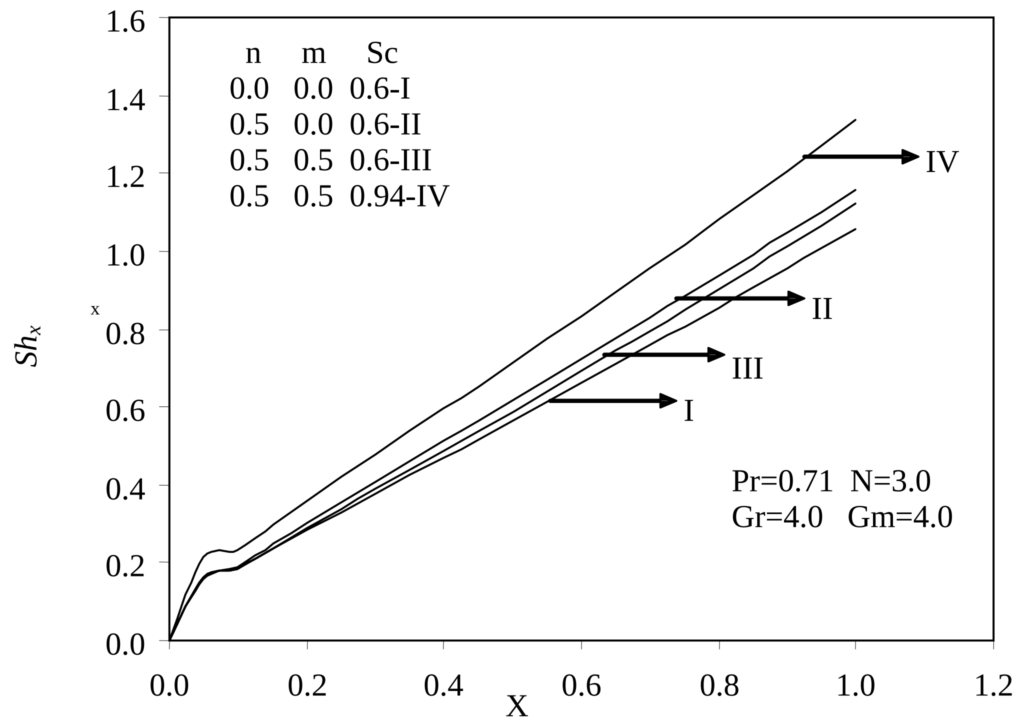

Fig.14 Local Sherwood number for different *n, m* and *N*

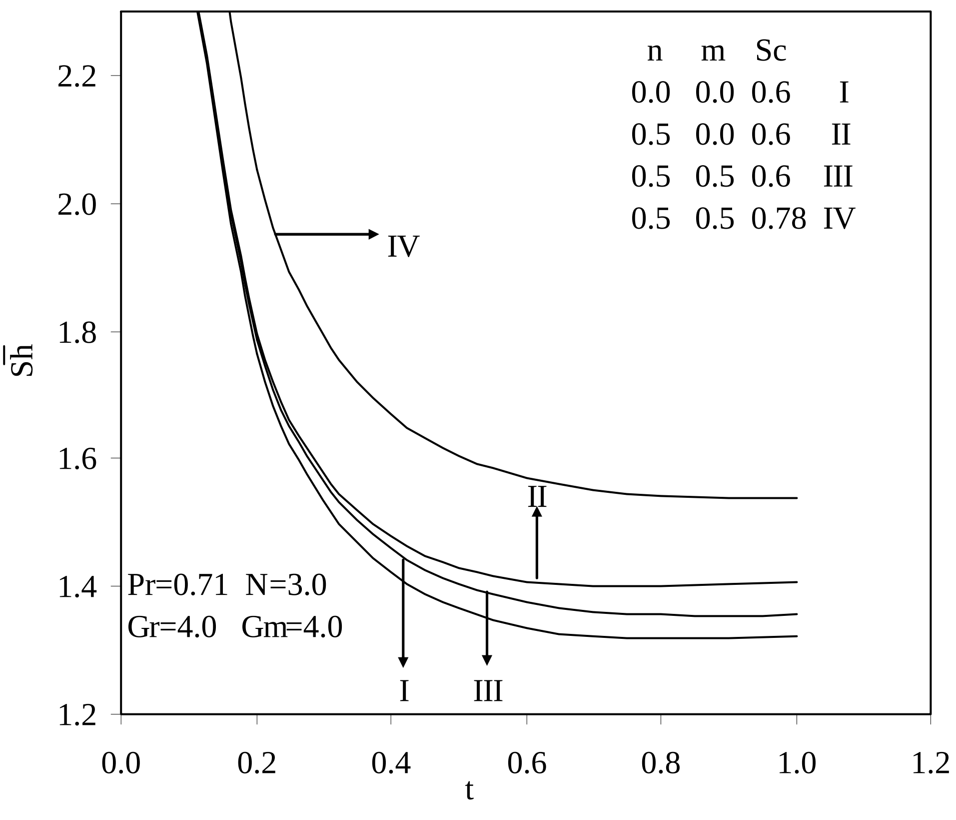

Fig. 15: Average Sherwood number for different values of *n, m* and *Sc*

The effect of radiation parameter *N* on the velocity and temperature variations is depicted in Figs.4 and 6. The radiation parameter *N* (i.e., Stark number) defines the relative contribution of conduction heat transfer to thermal radiation transfer. As *N* increases, considerable reduction is observed in velocity and temperature profiles from the peak value at the wall (Y = 0) across the boundary layer regime to the free stream (Y→ ∞), at which the velocity and temperature are negligible for any value of *N*. It is also observed that reduction in velocity and temperature are accompanied by simultaneous reductions in both velocity and thermal boundary layers.

The effect of magnetic parameter *M* on the steady state velocity and temperature near the plate are presented in Figs 4 and 8. Application of a transverse magnetic field to an electrically conducting flow gives rise to a resistive type of force called Lorenz force. This force has the tendency to slow down the motion of fluid in the boundary layer and to increase its temperature. As expected, as *M* increases the velocity decreases, whereas the temperature increases. The effect of *Pr* on the temperature profiles is shown in Fig.8. Prandtl number defines the ratio of momentum diffusivity to thermal diffusivity. It is noticed that the temperature decreases as *Pr* increases.

The effects of temperature exponent m, concentration exponent n and Eckert number *Ec* on the velocity and temperature are shown in Figs 5 and 7. An increase in the value of *m* or *n* reduces both the velocity and temperature. Eckert number designates the ratio of the kinetic energy of the flow to the boundary layer enthalpy difference. The effect of viscous dissipation on the flow field is to increase the energy, yielding a greater fluid temperature and as a consequence greater buoyancy force. The increase in the buoyancy force due to an increase in the dissipation parameter enhances the convective velocity and also the temperature.

The concentration profiles for different values of *m*, *n* and *Sc* are shown in Fig. 9. The concentration reduces with an increase in *m* or *n* or *Sc*.

The effects of *Sc, N, m* and *n* on the local skin-friction coefficient (τ_x) and the average skin-friction coefficient$(\bar{\tau})$ are shown in Figs. 10 and 11. It is noticed that, the local and average skin-friction coefficients decrease as *m* or *n* or *Sc* increases. It is also observed that, the local and average skin-friction coefficients increase as *N* increases.

The local Nusselt number (Nu_x) and the average Nusselt number $(\overline{Nu})$ for different *m, n* and *N* are shown in Figs 12 and 13. It is observed that, the local and average Nusselt numbers increase with an increase in *N* or *m* and they decrease with an increase in *n*. The effects of *m, n* and *Sc* on the local Sherwood number (Sh_x) and the average Sherwood number $(\overline{Sh})$ are shown in Figs 14 and 15. It is found that, the local and average Sherwood numbers increase with an increase in *n* or *Sc.*

5. Conclusions

A mathematical model has been presented for the radiative-convective flow in a gray absorbing-emitting fluid adjacent to an impulsively started vertical plate with variable temperature and concentration. From the study, following conclusions can be drawn:

1. An increase in radiation or exponents in power law variation of wall temperature and concentration reduces the velocity, temperature and concentration**.**
2. As the viscous dissipation increases, the velocity as well as the temperature increases.
3. The concentration reduces with an increase in *m* or *n* or *Sc*.
4. The local and average skin-friction coefficients decrease as *m* or *n* or *Sc* increases, whereas they increase as the radiation parameter increases.
5. The local and average Nusselt numbers increase as *N* or *m* increases and they decrease as *n* increases.
6. The local and average Sherwood numbers increase as *n* or *Sc* increases.

References

Abd-El-Naby, M.A., Elasayed, M.E., Elbarbary, Nader,Y. and Abdelzem. (2003): Finite Difference Solution Of Radiation Effects On MHD Free Convection Flow Over A Vertical Plate With Variable Surface Temperature, J.Appl. Math.,Vol. 2, pp. 65-86. doi:10.1155/S1110757X0320509X

Brewster, M.Q. (1992): Thermal Radiative Transfer And Properties, John Wiley & sons. Inc., New York.

Carnahan, B., Luther, H.A. and Willkes, J.O. (1969): Applied Numerical Methods, John Wiley & Sons, New York.

Chamkha A.J., Takhar H.S. and Soundalgekar V.M. (2001): Radiation Effects On Free Convection Flow Past A Semi-Infinite Vertical Plate With Mass Transfer, Chem.Engg.J., Vol.84, pp.335-342. doi:10.1016/S1385-8947(00)00378-8

Chaudhary. R. C., Bhupendra Kumar Sharma and Abhay Kumar Jha, (2006): Radiation Effect With Simultaneous Thermal And Mass Diffusion In MHD Mixed Convection Flow From A Vertical Surface With Ohmic Heating, Romanian Journal Of Physics, Vol.51. No. 7-8, pp. 715-727.

Israel-Cookey,C., Ogulu, A. and Omubo-Pepple. (2003): Influence Of Viscous Dissipation On Unsteady MHD Free Convection Flow Past An Infinite Vertical Plate In Porous Medium With Time-Dependent Suction, Int. J. Heat and Mass Transfer, Vol.46, pp.2305-2311.

doi:10.1016/S0017-9310(02)00544-6

Joaquin Zueco Jordan, (2007): Network Simulation Method Applied To Radiation And Dissipation Effects On MHD Unsteady Free Convection Over Vertical Porous Plate, Appl. Math. Modelling, Vol.31, pp.2019-2033. doi:10.1016/j.apm.2006.08.004

Mahajan, R.L, Gebhart, B.B. (1989): Viscous Dissipation Effects In Buoyancy-Induced Flows, Int. J. Heat Mass Transfer, Vol.32,No. 7, pp. 1380-1382. doi:10.1016/0017-9310(89)90038-0

Muthucumarswamy, R. and Senthil Kumar (2004): Heat And Mass Transfer Effects On Moving Vertical Plate In The Presence Of Thermal Radiation, Theoretical Applied Mechanics, Vol.31, pp 35-46. doi:10.2298/TAM0401035M

Ramachandra Prasad, V., Bhaskar Reddy, N. and Muthucumaraswamy, R.(2006): Finite Difference Analysis Of Radiative Free Convection Flow Past An Impulsively Started Vertical Plate With Variable Heat And Mass Flux, J. Appl. Theo. Mech., Vol.33, pp.31-63.

doi:10.2298/TAM0601031P

Ramachandra Prasad, V., Bhaskar Reddy, N. and Muthucumaraswamy, R. (2007): Radiation and Mass Transfer Effects On Two-Dimensional Flow Past an Impulsively Started Isothermal Vertical Plate, Int. Journal of Thermal Sciencess, Vol.46, No.12, pp.1251-1258.

doi:10.1016/j.ijthermalsci.2007.01.004

Takhar, H.S., Gorla, R.S.R and Soundalgekar, V.M.(1996): Radiation Effects On MHD Free Convection Flow Of A Radiating Fluid Past A Semi-Infinite Vertical Plate, Int. J. Numerical Methods for Heat and Fluid Flow, Vol.6, pp.77-83.